C2orf71 Mutations as a Frequent Cause of Autosomal-Recessive Retinitis Pigmentosa: Clinical Analysis and Presentation of 8 Novel Mutations

Christina Gerth-Kahlert,[1] Amit Tiwari,[2] James V. M. Hanson,[1] Vaishnavi Batmanabane,[3] Elias Traboulsi,[4] Mark E. Pennesi,[5] Abdullah A. Al-Qahtani,[5,6] Byron L. Lam,[7] John Heckenlively,[8] Sandrine A. Zweifel,[1] Ajoy Vincent,[3] Fabienne Fierz,[9] Daniel Barthelmes,[1] Kari Branham,[8] Naheed Khan,[8] Angela Bahr,[2] Luzy Baehr,[2] István Magyar,[2] Samuel Koller,[2] Silvia Azzarello-Burri,[10] Dunja Niedrist,[10] Elise Heon,[3] and Wolfgang Berger[2,11,12]

[1]Department of Ophthalmology, University Hospital Zurich, Zurich, Switzerland
[2]Institute of Medical Molecular Genetics, University of Zurich, Schlieren, Switzerland
[3]Department of Ophthalmology and Vision Sciences, The Hospital of Sick Children, Toronto, Canada
[4]Cole Eye Institute, Cleveland Clinic, Cleveland, United States
[5]Casey Eye Institute, Department of Ophthalmology, Oregon Health & Science University, Portland, Oregon, United States
[6]King Fahd University Hospital, University of Dammam, Dammam, Saudi Arabia
[7]Bascom Palmer Eye Institute, Miami, United States
[8]University of Michigan Department of Ophthalmology and Visual Sciences, Ann Arbor, Michigan, United States
[9]Eye Clinic, Lucerne Cantonal Hospital, Lucerne, Switzerland
[10]Institute of Medical Genetics, University of Zurich, Schlieren, Switzerland
[11]Zurich Center for Integrative Human Physiology, University of Zurich, Zurich, Switzerland
[12]Neuroscience Center Zurich, University and ETH Zurich, Zurich, Switzerland

Correspondence: Christina Gerth-Kahlert, Department of Ophthalmology, University Hospital Zurich, Frauenklinikstrasse 24, 8091 Zurich, Switzerland; christina.gerth-kahlert@usz.ch.

Submitted: February 1, 2017
Accepted: June 13, 2017

Citation: Gerth-Kahlert C, Tiwari A, Hanson JVM, et al. *C2orf71* mutations as a frequent cause of autosomal-recessive retinitis pigmentosa: clinical analysis and presentation of 8 novel mutations. *Invest Ophthalmol Vis Sci*. 2017;58:3840–3850. DOI:10.1167/iovs.17-21597

Purpose. To define the phenotype of *C2orf71* associated retinopathy and to present novel mutations in this gene.

Methods. A retrospective multicenter study of patients with retinopathy and identified *C2orf71* mutations was performed. Ocular function (visual acuity, visual fields, electroretinogram [ERG] responses); retinal morphology (fundus, optical coherence tomography); and underlying mutations were analyzed.

Results. Thirteen patients from 11 families, who were aged 7 to 63 years (mean: 32.1 years) at their first examination with presumed compound heterozygous (6/13 patients) or homozygous (7/13 patients) *C2orf71* mutations were identified. Eight of the mutations were novel. Truncation mutations were responsible in all cases. Nyctalopia was observed in less than 50% of patients. Visual acuity ranged from 20/20 to light perception. Severe visual loss was associated with atrophic maculopathy. Full-field ERG responses showed severe progressive cone-rod or rod-cone dysfunction. Typical fundus changes were progressive symmetrical retinopathy with an early mild maculopathy and patchy circular midperipheral RPE atrophy. Normal retinal lamination was preserved despite early disruption of the ellipsoid zone and RPE irregularities. Outer retinal tubulations were associated with better-preserved visual acuity.

Conclusions. On the basis of our multicenter analysis, *C2orf71* might represent a more frequently mutated gene in autosomal recessive retinitis pigmentosa in some populations. The phenotype analysis over a wide age range showed a variable and progressive retinal degeneration with early onset maculopathy and a better visual potential before the age of 30 years.

Keywords: *C2orf71* gene, retinitis pigmentosa, phenotype, outer retinal tubulation

The human gene *C2orf71* consists of two exons and codes for an open reading frame of 1288 amino acid residues. Expression studies in the Zebrafish model showed that the protein is localized in primary cilia. This could be suggestive for a role of the protein in the outer segments of photoreceptor cells or in the connecting cilium.[1]

Mutations in *C2orf71* were first described in 2010 in six patients with nonsyndromic, autosomal-recessive retinitis pigmentosa (arRP) and two patients with early onset retinal dystrophy with nystagmus.[1] The current total number of mutations in the Human Gene Mutation Database (HGMD) is 35 (13 missense, 11 nonsense, 9 small deletions, 1 insertion, and 1 insertion/deletion). In the majority of patients, mutations lead to RP, but other phenotypes (such as cone-rod dystrophy) have also been reported. The frequency of *C2orf71* mutations and related phenotypes appear to vary between populations.

For example, in Swiss patients with retinal dystrophies, the frequency of pathogenic sequence variations in *C2orf71*is 15%,[2] but it is only 1% in French patients with autosomal-recessive RP.[3] Audo et al.[3] identified two patients with marked macular atrophy and severe retinal dysfunction at age 34 and 44 years. Collin et al.[4] reported a phenotype of RP with early onset cone dysfunction in one family of four affected individuals between 30 and 37 years old, while two other families showed "typical signs of RP" and severe retinal dysfunction. Since then, isolated or familial cases with *C2orf71* mutations associated with a RP phenotype have been documented.[5–11]

In this study, we present the clinical and genetic findings in the largest cohort to date of 13 patients with a wide age range and eight novel mutations in order to better characterize *C2orf71*-associated phenotypes.

Methods

This is a retrospective multicenter study, which was approved by the respective ethics board of each institution and met the tenets of the Declaration of Helsinki. Data were collected from six different institutions. The inclusion criterion was the clinically approved molecular diagnosis of presumably pathogenic *C2orf71* mutations in individuals affected with retinal dysfunction.

Ocular Function and Morphology

All subjects had attended an ocular genetics clinic and received an eye examination, including dilated fundus examination; visual acuity (VA) measurement using Snellen or Early Treatment Diabetic Retinopathy Study (ETDRS) charts; fundus photography and fundus autofluorescence (FAF; Spectralis; Heidelberg Engineering, Heidelberg, Germany; Visucam$^{NM/FA}$; Carl Zeiss Meditec, Jena, Germany; or Optomap; Optos, Dunfermline, UK). Spectral-domain optical coherence tomography (SD-OCT; Heidelberg Engineering; Cirrus; Carl Zeiss Meditec) was not available for cases with poor central fixation. When possible, OCT volume scans were centered on the retinal location used for fixation; line scans were centered at the fovea. Central retinal thickness (CRT) and total macular volume (TMV; employing the 1, 2.22, 3.45 mm ETDRS grid centered on the fovea) were measured using the proprietary OCT software. Full-field (ff) and multifocal (mf)ERGs were recorded according to International Society for Clinical Electrophysiology of Vision standards[12,13] using an Espion system (Diagnosys LLC, Lowell, MA, USA); the LKC system (LKC Technologies, Inc. Gaithersburg, MD, USA); or a custom ERG system.[14] Full-field ERG was available in all but three patients. Multifocal ERG using a 103- or 61-hexagon stimulus array was possible in five patients who were able to maintain steady central fixation. Optical coherence tomography and ERG data were compared with age-matched normal values. Kinetic visual fields were measured using the Goldmann perimeter or the Octopus 900 perimeter (Haag Streit AG, Switzerland).

Molecular Genetic Testing

Genetic testing was performed by high throughput, next generation DNA sequencing using different platforms and strategies from Clinical Laboratory Improvement Amendments–approved laboratories (panel or whole exome sequencing). Bioinformatic data analysis, variant prioritization, and confirmation of identified variants were done by Sanger sequencing.[2]

Results

Thirteen patients (seven female and six male) from 11 families were identified with compound heterozygous (6/13 patients) or homozygous (7/13 patients) mutations in the *C2orf71* gene. Consanguinity was identified in one family (ID# 13). The only two families with two affected children were from Switzerland and without known consanguinity or common ancestry. Caucasian ethnicity was documented or presumed in 9 of 12 patients, with an additional patient being of mixed Caucasian/Native American descent. One patient was of Korean and one of mixed Lebanese/Armenian descent. No ethnicity was recorded for the single remaining patient.

The mean age at which the clinical information was documented was 32.1 years (range: 7–63 years). The main symptom prompting the patients to seek an ophthalmologic examination was reduced vision, with 6 of 12 (one not documented) reporting nyctalopia. Awareness of nyctalopia was reported during the second decade while symptoms of photophobia were always denied. Myopia (mean: –4.4 diopters (D); range: –2.5 to –7.6 D) was observed in 8 of 12 patients.

Visual Function

Visual acuity ranged from 20/20 to light perception. Patients typically maintained good central visual function with visual acuity up to 20/40 or better in their third decade; however, four patients (ID# 3, 4, 5, 6) experienced severe visual loss in their third decade, from losing the ability to drive a car to counting fingers or light perception. All of these four patients described this vision loss as rapid over the course of a few years. An atrophic maculopathy was observed in all four cases.

Visual field analysis showed concentric constriction initially of the small isopters at ages 13 to the mid-20s, progressing to ring scotomas and severely reduced visual fields after the age of 30 years.

Retinal function measured by ffERG in 11 patients showed early impairment of both rod and cone function pointing to severe retinal dysfunction, including at the youngest age recorded (15 years; ID# 1, 11). These ERG changes were variable, with cone more than rod dysfunction in three patients where test results are available from a younger age (ID# 2, 11, 13) whereas other patients show equally reduced and delayed rod and cone responses. The results of patients tested at an older age (ID# 3, 5, 12) showed preferential reduction and delay of the rod system or nonrecordable responses. The youngest age at which ffERG responses were no longer recordable was 26 years (ID# 6). Multifocal ERG recordings were abnormal in all five available patients as early as age 15 years. In two patients (ID# 1, 2), mfERG testing was performed twice, showing progressive loss of cone-mediated macular function.

Retinal Morphology

Analysis of the 13 patients (including retinal assessments from previous clinical examinations not shown here) shows a progressive and symmetrical retinopathy starting with an early mild maculopathy with a tapetoretinal sheen and wrinkling of the internal limiting membrane. Patchy circular retinal RPE atrophy was typically found in the midperipheral retina, and may be placoid in appearance; however, bone spicule pigmentation was rarely observed during the entire disease course. Late-stage disease as diagnosed at age 32 (ID# 5) is marked by extensive macular and peripheral chorioretinal retinal atrophy with waxy optic discs. Intra- and interfamilial variability in the severity of the phenotype was observed.

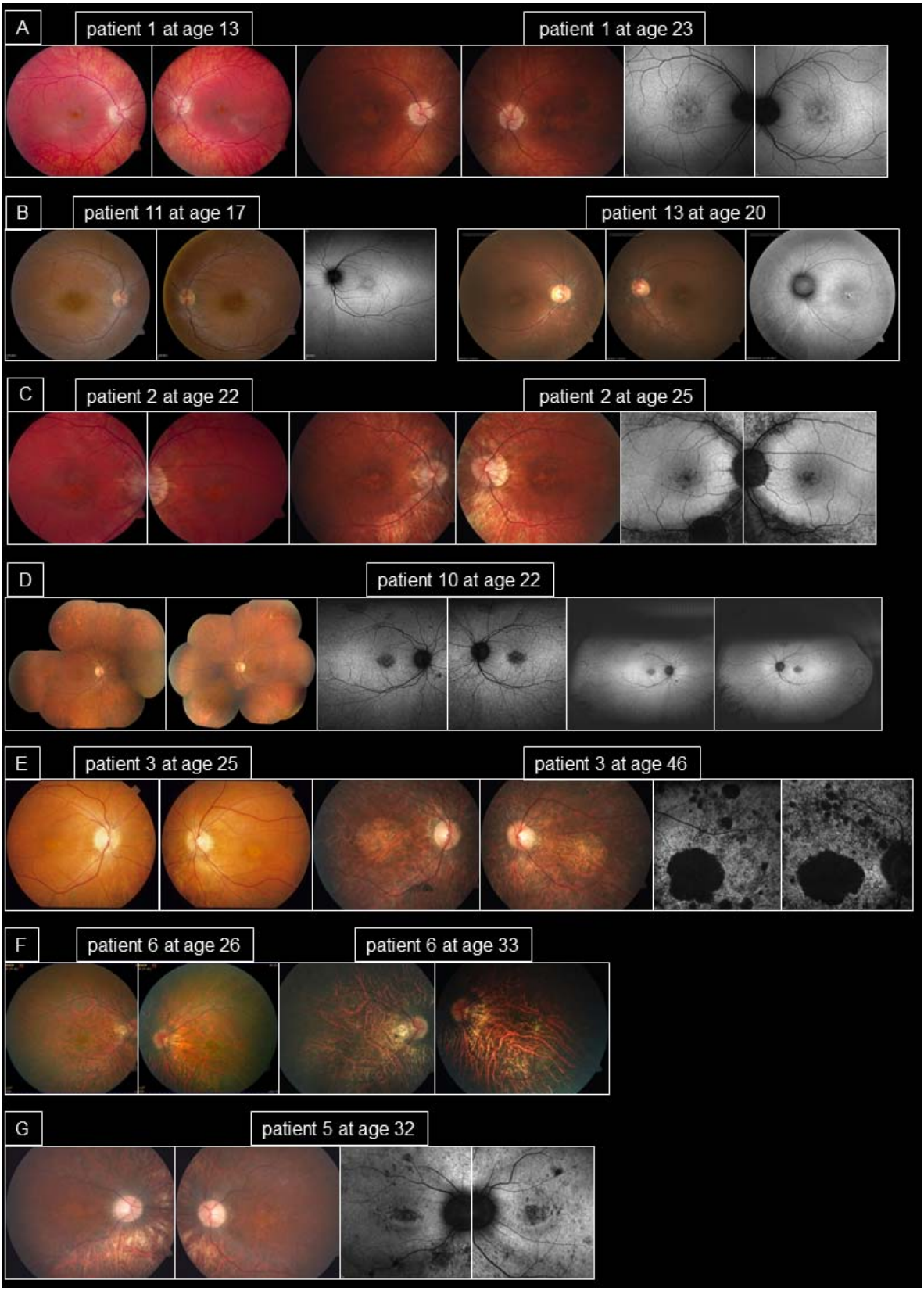

Figure 1. Fundus photographs and corresponding AF images (when available) of all patients arranged by age. Comparison of fundus images of patient #1 at ages 13 and 23 years demonstrate a progressive maculopathy and speckled macular AF at age 23. (**A**) Fundus images of patients #11 and 13 at age 17 and 20 years, respectively, show a mild maculopathy and corresponding central hypo-AF with surrounding hyper-AF (left eye AF not shown). (**B**) Fundus images from patient #2 at age 22 and 25 years show a maculopathy and atrophic areas along the vascular arcade as well as hypo-AF at age 25. (**C**) Panoramic fundus images of patient #10 at age 22 years illustrate mild maculopathy and speckled hypo AF. (**D**) A severe maculopathy is visible on fundus images of patient #3, progressively worsening between ages 25 and 46 years. AF images show reduced AF in the

Investigative Ophthalmology & Visual Science

atrophic area and hypo- and hyper-AF over the entire fundus area imaged at age 46 years. (**E**) A progressive maculopathy and myopic optic disc changes are shown in patient #6 at ages 26 and 33 years. (**F**) Maculopathy and midperipheral chorioretinal atrophy are shown in patient #5 at age 32 years. Corresponding AF demonstrates macular hypo-AF with a surrounding ring of hyper-AF and speckled hypo AF at the posterior pole. (**G**). Scattered punctate deposits and patchy atrophy are visible in fundus images of patient #12 at age 44 years. Wide field AF shows extensive macular hypo-AF with peripheral speckled hypo-AF sparing the midperiphery. (**H**) Advanced macular atrophy with extensive hypo-AF is shown in patient #7 at age 44. (**I**) Optic atrophy, chorioretinal atrophy, and hypo-AF are visible in patient #9 at age 47 years. (**J**) Extended chorioretinal atrophy but relatively preserved optic disc is shown in the fundus images of patient #4 at age 50. (**K**) Placoid chorioretinal atrophy with thinned vessels and waxy optic disc and large areas of hypo-AF are present on patient #8 at age 63 years (**L**).

The autofluorescence (AF) in *C2orf71*-related retinal dystrophy shows perifoveal to macular hypo- and hyper-AF rings at early stages (Fig. 1). At later disease stages, hypo-AF is typically seen in areas of RPE atrophy. Spectral-domain OCT demonstrates normal retinal lamination, but early disruption of the ellipsoid zone and RPE irregularities (Fig. 2). Retinal layer attenuation and reduced image quality due to eye movements precluded reliable layer identification and quantification in all but one patient. Manual retinal layer segmentation was only possible on images obtained in one patient (ID# 2 at age 25) that were compared with age-matched control data. Those images revealed thinned inner and outer retinal layers without a predilection of a specific retinal layer; therefore, segmentation supported the qualitative assessment of preserved but universally thinned structure of the retinal layers. Analysis of total macular volume (TMV) in both eyes of six patients aged 23 to 63 years, and with early to advanced disease stages, showed a significant reduction even at a young age of 23 years. Central retinal thickness (CRT) was less reduced compared to TMV. Within the 3rd and 4th decade, CRT values demonstrated

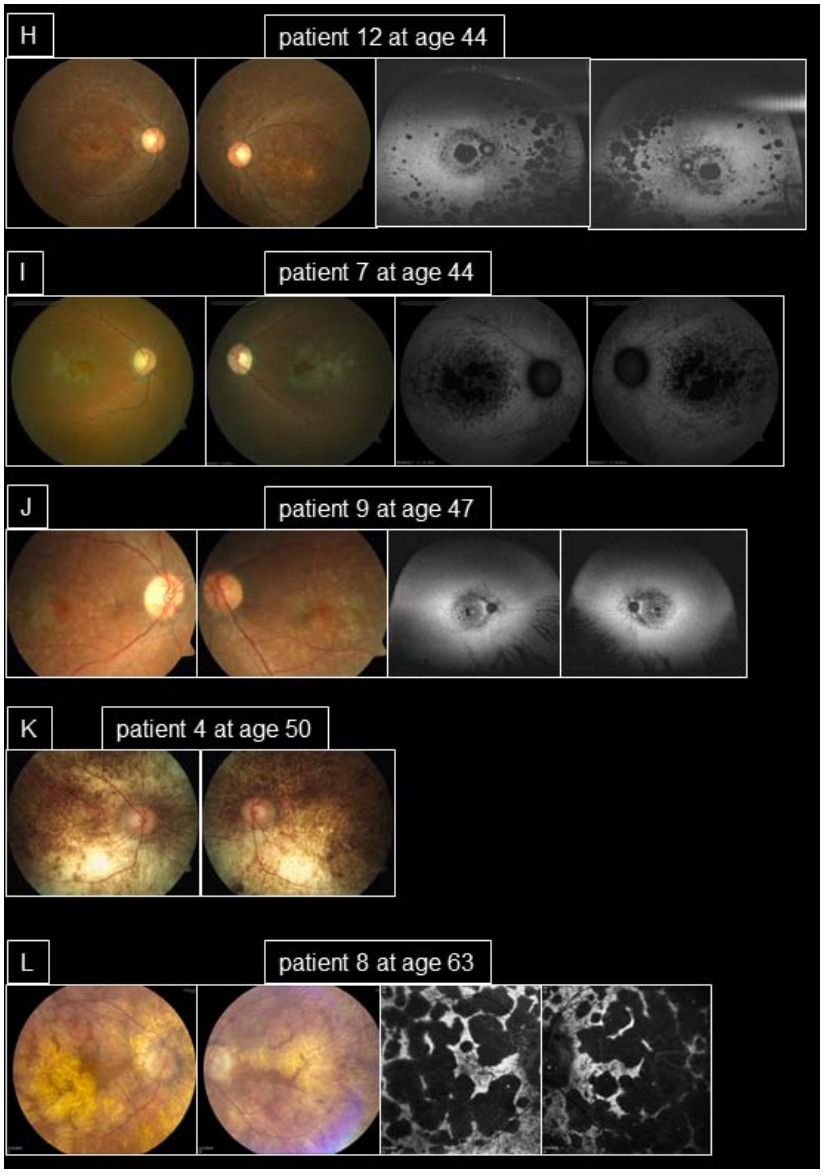

Figure 1. Continued.

Investigative Ophthalmology & Visual Science

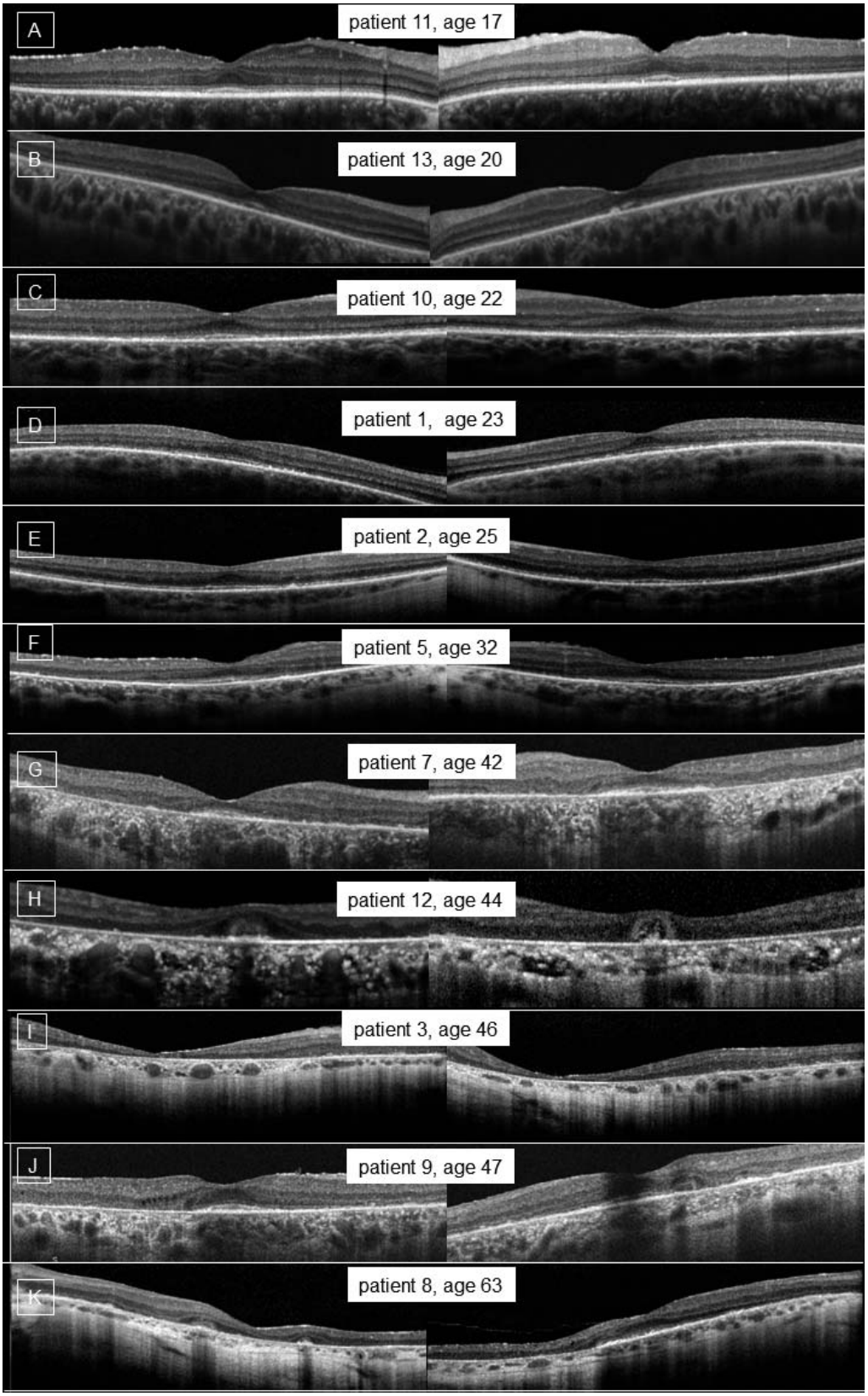

Figure 2. Spectral-domain OCT images of patients studied presented by eye pair in the order of age at imaging. Outer retinal dystrophy with thinning of the photoreceptor layers, advancing with age, is demonstrated (**A–L**). Outer retinal tubulations are visible in the outer retina subfoveally (both eyes of patient #12 [**H**]); extrafoveally (left eye of patient #9 [**J**]). (**J**) Open ORTs lacking a hyperreflective border on their outer aspects are present in patient #9. (**K**) A so-called "forming ORT" with a free edge scrolling is visible in the left eye of patient #8.

Investigative Ophthalmology & Visual Science

Figure 3. Macular volume and central retinal thickness as a function of age in patients with *C2orf71* mutations showing significant volume reduction in the presence of variable central thickness. *Gray lines* show the 5% and 95% confidence interval of normative data.

a slight to severe reduction as plotted in Figure 3. Abnormal subfoveal changes in the outer retina were observed in both eyes of patient #12 by SD-OCT. The ovoid tubular structures with a partial hyperreflective border are visible within the foveal region and resemble the previous description of photoreceptor rosettes[15] or outer retinal tubulation (ORT).[16] Hyperreflective material within the ORT lumen was identified in the left eye of patient #12. This could indicate preserved inner segment ellipsoids and trapped retinal pigment.[17] Note that the tubular structures shown in Figure 2 lack hyperreflectivity on their outer aspects and are therefore called open ORT. Extrafoveal open ORTs were visible in two other patients (ID# 8, 9). In patient #9, the subfoveal OCT cross-section shows a forming tubulation.

Mutational Analysis

We identified presumable compound heterozygous mutations in six patients and presumable homozygous mutations in seven patients in the *C2orf71* gene. Eight of the mutations were novel and seven have been described previously[2–4,18,19] (Table 1). All of the 26 mutant alleles were truncation mutations (stop gain, frameshift deletions, or insertions). This is consistent with the high number of truncation mutations previously identified in *C2orf71* in retinal dystrophy patients (Source: HGMD Professional).

Segregation Analysis

Segregation analysis was available in seven patients of five families. In family 1, the mutations c.1709_1728del and c.2227_2228del were identified in the unaffected mother and

Table 1. Summary of Mutation Information and Demographics

Family ID	Patient ID	Lab ID Number	Allele 1 cDNA, Reference	ExAC Allele Frequency (%)	Allele 1 Protein	Allele 2 cDNA, Reference	ExAC Allele Frequency, %	Allele 2 Protein	Segregation Analysis	Origin/Ethnicity	Sex
1	1	25999	c.1709_1728del (2)	–	p.Gly570GlufsTer3	c.2227_2228del (2)	–	p.Leu744GlufsTer7	+	Swiss	M
1	2	71703	c.1709_1728del (2)	–	p.Gly570GlufsTer3	c.2227_2228del (2)	–	p.Leu744GlufsTer7	+	Swiss	M
2	3	29870	c.1709_1728del (2)	–	p.Gly570GlufsTer3	*	–		+	Swiss	F
2	4	29868	c.1709_1728del (2)	–	p.Gly570GlufsTer3	*	–		+	Swiss	M
3	5	71918	c.3002G>A (3)	0.0034	p.Trp1001Ter	*			–	Kosovo	F
4	6	70052	c.1949G>A (18)	0.0025	p.Trp650Ter	*			–	Croatia	M
5	7	01_c2orf71	c.920T>A*	–	p.Leu307Ter	*			–	Italian	F
6	8	–	c.3604C>T*	0.001	p.Arg1202Ter	c.402_405del*	–	p.Ser134ArgfsTer47	–	Caucasian	M
7	9	–	c.1273C>T (19)	–	p.Arg425Ter	c.3002G>A (3)	0.0034	p.Trp1001Ter	–	Caucasian?	F
8	10	CEI24082	c.1206_1207dup*	–	p.Cys403SerfsTer47	c.1206_1207dup*	–	p.Cys403SerfsTer47	+	Caucasian/Native American	F
9	11	4651	c.2756_2768del (4)	–	p.Lys919ThrfsTer2	c.802C>T*	–	p.Gln268Ter	+	Lebanese/Armenian	M
10	12	CEI24387	c.1837C>T*	0.0017	p.Arg613Ter	c.3358_3359del*	–	p.His1120PhefsTer12	–	Korean	F
11	13	03_c2orf71	c.478_479insA*	–	p.Cys160Ter	c.478_479insA*	–	p.Cys160Ter	+	N/A	F

N/A, not available.

* Novel mutations. If only allele 1 is indicated in a patient, genetic analysis had revealed homozygosity for this allele and the parents were not available for testing in order to confirm that both alleles are carrying the same mutation.

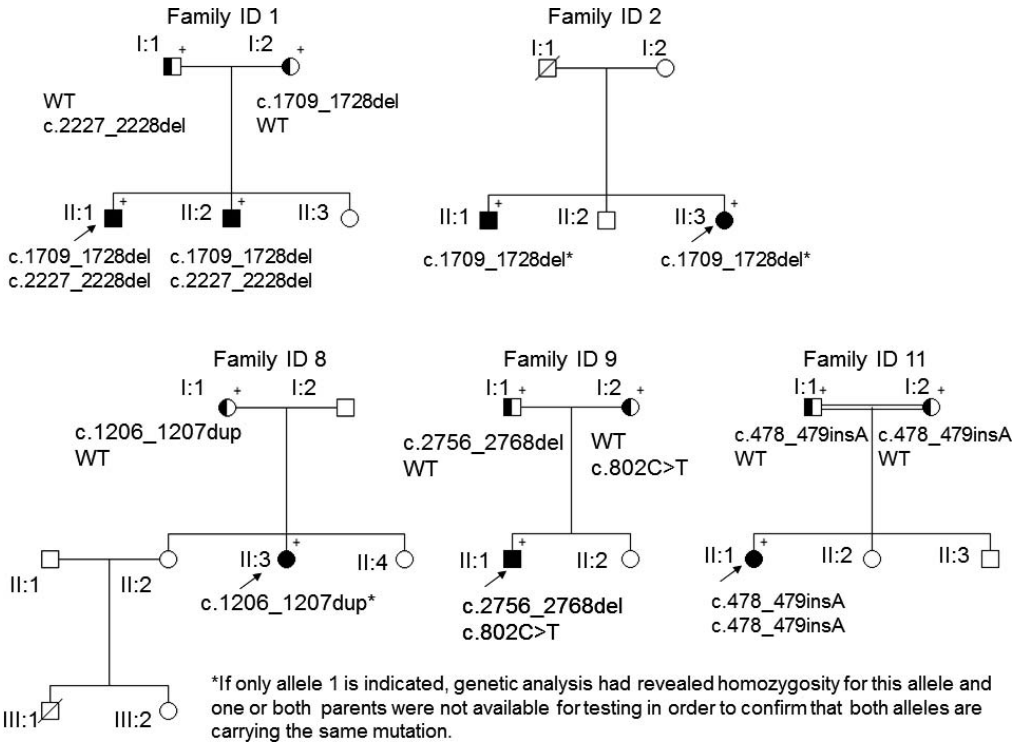

Figure 4. Pedigrees and segregation of available families (families 1, 2 8, 9, and 11).

father, respectively. In family 2, both identified mutations cosegregated with the disease and no unaffected family member was available for testing. The mutation c.1206_1207dup was identified in a heterozygous state in the unaffected mother of patient #10. Other unaffected family members (father and two siblings) were not available for testing. The mutation c.2756_2768del was identified in the unaffected father and the novel mutation c.802C>T was identified in the unaffected mother of patient #11.

The novel mutation c.478_479insA was identified in the unaffected mother and father of patient #13.

Haplotype Analysis Indicates Common Ancestry

The sequence variation NM_001029883.2: c.1709_1728del (p.Gly570GlufsTer3) was identified in four Swiss patients from two families (families 1 and 2), which suggests it to be more abundant in the Swiss population. A common ancestry of these patients could not be ascertained by information provided by the patient's family. Haplotype analysis in one affected patient of one member of both family 1 (patient ID# 2; lab ID# 71703) and family 2 (patient ID# 3; lab ID# 29870) supported the *C2orf71* location on the "p" arm of chromosome 2. This analysis also revealed interesting results: out of 134 variants in 29,870 and 144 variants in 71,703 in RD genes on the "p" arm of chromosome 2, 70 variants were common in both patients (data not shown), in addition to the pathogenic frameshift deletion. The sharing of almost of 50% of these variants in the respective region is indicative of a shared ancestry in the two patients and therefore two families of four affected patients.

Discussion

This is the largest case series providing a detailed *C2orf71* associated retinopathy phenotype characterization of the *C2orf71*-associated retinopathy in 13 patients over a wide range of ages. In all cases, *C2orf71* mutations were associated with signs and symptoms reminiscent of RP, except for the fact that all had an early maculopathy and that less than half complained of nyctalopia. Early macular pathology with cone-mediated dysfunction was associated with reduced vision at an early disease stage. Follow-up data were available only in a few individual patients.

The spectrum of changes seen on fundus appearance, as demonstrated in Figure 1, ranges from early onset maculopathy (patients #1, 2, and 11) to RP-like (e.g., patients #6, 10, and 12) or choroideremia-like (patients #4 and 8) chorioretinal changes. Microstructural loss of photoreceptor integrity and retinal layer atrophy with maintained laminar structure, even in the late stages of disease, point to a primary photoreceptor disease process. The degenerative sign of ORT in the region of less severely affected central macula or at the "junctional zone" of advanced to less-advanced disease severity was identified in three of the reported patients. Outer retinal tubulations have been described in various retinal degenerative disorders and can be found in closed and open forms.[16,20–24] Analysis by SD-OCT and adaptive optics imaging together with histopathologic studies point to degenerative cones with remnant or absent outer segments and inner segments with small and dispersed organelles as a source of high reflectivity around the ORT.[15,17,21,25] It is proposed that the rosette arrangement promotes survival of degenerative photoreceptor cells.[16] It is of particular note that visual acuity appears to be less reduced in all three patients with visible ORT, despite the older ages of these patients relative to the cohort as a whole. Hyperreflective material within the ORT lumen is one of the major features of ORT and could be identified in one patient (#12). These luminal contents may indicate preserved inner segment ellipsoids. The subfoveal location of the ORT in patient #12 could potentially explain the preserved visual acuity in this patient. Histologic studies have shown the presence of RPE and other cells within the ORT lumen, which might provide trophic support to photoreceptors.[21]

Table 2. Summary of Ocular Phenotype in Patients Studied (Arranged by Age)

Family ID	Patient ID	Age at 1st Visit, y	Age at Last Visit, y	VA First Visit		VA Last Visit		Nyctalopia	Refraction, MSE		Age at VF	VF	Ages at ERG, y	ffERG	mfERG
				RE	LE	RE	LE		RE	LE					
1	1	13	23	20/30	20/30	20/50	20/40	-	−7,6	−3	23	Slight constriction (i4e: 5°–10°)	15/23	(1) Scotopic & photopic: severely reduced, (2) progressive reduction and delay	Severely reduced to NR
9	11	15	20	20/30	20/30	20/20	20/25	-	0,4	0,8	15	Concentric constriction to smaller isopters	15	Scotopic < photopic severely reduced and delayed	Severely reduced
11	13	20	-	20/32	20/32	-	-	+	−4	−2,9	20	Normal	20	Scotopic severely reduced, photopic NR	N/A
1	2	22	25	20/25	20/25	20/30	20/30	-	−4,4	−5,5	25	Constriction (i4e: 35°), midperipheral scotoma	22/25	(1) Scotopic and photopic: severely reduced and delayed, (2) scotopic: progressive reduction and delay, photopic NR	NR
8	10	22	26	20/30	20/40	20/30	20/40	-	0	0	26	Slight constriction (I2e: 10°) relative mid-peripheral scotoma	22/26	Scotopic and photopic severely reduced	Severely reduced and delayed
2	3	25	46	20/25	20/25	LP	LP	+	Myopia	Myopia	25	Slight constriction (III4e: 70°), midperipheral scotoma	25/31	(1) Scotopic: NR, photopic: severely reduced; (2) NR	N/A
4	6	7,5	33	20/25	20/30	CF	CF	-	−7	−6,5	26	severe constriction (V4e: 45°)	26	NR	N/A
3	5	32	-	20/200	20/400	-	-	+	−2,5	−1,3	32	Not reliable	32	Scotopic: NR, photopic: severely reduced and delayed	NR
10	12	34	44	20/40	20/40	20/40	HM	+	−3	−5	44	Severe constriction 5° (largest target) RE, N/A LA	34/37	Scotopic: NR, photopic: severely reduced	N/A
5	7	42	44	20/80	20/50	20/50-2	20/50	+	N/A	N/A	42	Severe constriction (3° RE, 15° LE)	42	NR	N/A
7	9	47	47	20/25	20/30	20/25	20/25	+	0.5	0,5	47	Ring scotoma	N/A	N/A	N/A
2	4	50	-	LP	LP	-	-	-	Myopia	Myopia	N/A	N/A	50	NR	N/A
6	8	63	-	20/70	20/80	-	-		N/A	N/A	N/A	N/A	N/A	N/A	N/A

HM, hand motion detection; LE, left eye; LP, light perception; MSE, mean spherical equivalent; NR, nonrecordable; RE, right eye; VF, visual fields (horizontal for listed isopter).

Table 3. Descriptive Summary of Retinal Changes in Patients Studied

Family ID	Patient ID	Age at Exam, y	Maculopathy	Fundus Periphery	AF	Age at SD-OCT, y	ORT	SD-OCT CRT, µm		SD-OCT TMV, mm³	
								RE	LE	RE	LE
1	1	13/23	+ (f/u ++)	Midperipheral RPE atrophy	Macular speckled hypo/ hyper AF	23	-	208	202	2.53	2.46
9	11	17	+	Normal	Perifoveal speckled hypo/ hyper AF	17	-	N/A	N/A	N/A	N/A
11	13	20	+	Midperipheral atrophy, some bony spicules	Peripheral speckled hypo AF	20	-	N/A	N/A	N/A	N/A
1	2	22/25	++	Midperipheral RPE atrophy	Perifoveal and midperipheral speckled hypo/ hyper AF	25	-	243	228	2.73	2.66
8	10	22	+	Midperipheral yellow/ white deposit with sparse pigment	Perifoveal speckled hypo/ hyper AF	22	-	215	221	3.05	2.99
2	3	25/46	+ (f/u +++)	Midperipheral partially circular RPE atrophy	Macular large hypo-AF area, speckled hypo-/hyper-AF reaching outside vascular arcade	46	-	66	49	1.87	1.81
4	6	26/33	+ (f/u ++)	Midperipheral atrophy, some bony spicules	N/A	N/A	-	N/A	N/A	N/A	N/A
3	5	32	++	Midperipheral atrophy	Macular and midperipheral speckled hypo/ hyper AF	32	-	195	197	2.45	2.55
10	12	44	++	Scattered deep punctate deposits and patchy atrophy	Macular: large hypo AF area, sparing small patch in center peripheral: speckled hypo-/hyper-AF, sparing the midperiphery	44	+	103	107	2.07	2.16
5	7	44	+++	Severe peripheral atrophy with pigment	Macular and midperipheral speckled hypo/ hyper AF	42	-	N/A	N/A	N/A	N/A
7	9	47	++ (RE ERM)	Inferior circular chorioretinal atrophy, hypopigmented spots throughout fundus, waxy pallor of optic nerve head	Macular and nasal patchy hypo AF reaching to the vascular arcades	47	+	N/A	N/A	N/A	N/A
2	4	50	+++	Widespread chorioretinal atrophy	N/A	N/A	-	N/A	N/A	N/A	N/A
6	8	63	+++	Placoid-appearing atrophy, waxy pallor of optic nerve head	Large patches of hyper AF	63	+	210	115	2.18	1.99

BE, both eyes; CME, cystoid macular edema; ERM, epiretinal membrane; f/u, follow up examination.

Although visual deterioration usually occurs in the second to third decade, some useful vision can be retained up to the fifth or sixth decade. Advanced retinal dysfunction, as evidenced by ERG findings, was present at the first visit, indicating early disease onset, even before symptoms lead patients to seek medical attention. The electroretinogram results in our patient cohort point to an early-onset severe reduction of rod-cone or cone-rod function. This supports a previous report by Hebrard et al.[5] where two patients had onset of symptoms during the third decade together with documentation of severely abnormal ERG responses and a visible maculopathy. Retinal dysfunction seems to be more pronounced in the cone- than in the rod-driven pathway at a younger age, which was also observed in the recordable ERG data by others.[4–6] However, the very low response amplitudes available in our data set are insufficient to predict which photoreceptor pathway, cone- or rod driven, is more affected at an early age (such as in the first decade). Macular cone function might be earlier affected and more vulnerable than peripheral cones, which would explain the severely reduced mfERG responses and reduction in visual function. Earlier disease detection together with efficient and widely available molecular genetic testing will guide the understanding of *C2orf71*-related retinal dysfunction throughout its natural course.

The C2orf71 protein localization within the photoreceptor outer segments or connecting cilium[1] likely explains the photoreceptor degeneration as seen in several other ciliopathies, syndromic or not. Ciliopathies can range from severe morphogenic malformations to nonsyndromic early or late onset with photoreceptor degeneration.[26] The spectrum of retinal degeneration in ciliopathies is variable, including severe congenital dysfunction such as Leber congenital amaurosis (LCA) caused by mutations in *CEP290,* and progressive moderate to severe visual dysfunction (Usher syndrome, Bardet-Biedl syndrome, X-linked RP caused by *RPGR* mutation). The systemic signs observed in other ciliopathies (e.g., digit or kidney anomalies, hearing, neurological or cognitive impairment)[2728,29] have to date not been recorded in patients with *C2orf71* mutations.

Expression of *C2orf71*is restricted to the photoreceptors and the protein includes a 72–amino acid long proline-rich domain at the carboxyl terminus. These properties are quite similar to another retinal dystrophy associated gene *AIPL1,* which is associated with juvenile RP, LCA, and cone-rod dystrophy. Such domains have been shown to play important roles as common binding motifs and in biological processes involving rapid exchange and involvement of several proteins such as signaling cascades and transcription.[30]

We found eight novel mutations in *C2orf71*, all of which are nonsense or frameshift mutations. Consistent with published data, the mutations reported in this study comprise protein truncation mutations such as nonsense mutations and frameshift deletions and insertions. Interestingly, all of these mutations occurred in exon 1 of the gene. The nonsense and frameshift mutations are predicted to lead to nonsense-mediated decay. All cases were presumably or confirmed homozygous or compound heterozygous for nonsense and/or frameshift mutations. Thus truncating mutations, most likely leading to nonsense mediated decay of the messenger RNA, are the predominant pathogenic DNA sequence variation type in this study (>86%). This is higher than published numbers (HGMD Professional), in which about 67% of pathogenic sequence variants lead to truncating variations. There was no obvious genotype-phenotype correlation difference within the patients with truncating mutations. The majority of *C2orf71* mutations reported to date have been identified in Caucasian patients. To our knowledge, this is the first report of *C2orf71* mutations in a Korean patient.

In summary, this is the largest series of patients ($n = 13$) with *C2orf71*-related retinopathy in which eight novel *C2orf71* mutations were identified and the related structural and functional phenotypes defined. Together with 35 previously reported mutations entered in HGMD, *C2orf71* might represent one of the more frequently mutated gene in autosomal recessive RP, preceded by *EYS*, *USH2A*, *CRB1*, and *PDE6B*, making it more frequent than the contribution of mutations in *RPE65*, *ABCA4* (not including the 'classic' Stargardt phenotype), *MERTK* or *TULP1* in some populations such as in Switzerland. Although no pathognomonic features were identified, all patients had a slowly progressive photoreceptor degeneration with an early onset maculopathy and structural changes such as ORT. Useful vision is usually preserved until the 30s and may be preserved longer in some cases. These findings may have implications for potential therapeutic approaches; treatment before the age of 25 will likely offer the best opportunities as the central visual function deteriorates quickly afterwards.

Acknowledgments

Supported by the Mira Godard research fund and the McLaughlin Foundation (EH); a grant from the Swiss National Science Foundation (Grant Number: 320030_138507); Velux Stiftung Switzerland (WB); and in part by the Clinical Research Priority Program of the University of Zurich (JVMH).

Disclosure: **C. Gerth-Kahlert**, None; **A. Tiwari**, None; **J.V.M. Hanson**, Biogen (R); **V. Batmanabane**, None; **E. Traboulsi**, None; **M.E. Pennesi**, None; **A.A. Al-Qahtani**, None; **B.L. Lam**, None; **J. Heckenlively**, None; **S.A. Zweifel**, None; **A. Vincent**, None; **F. Fierz**, None; **D. Barthelmes**, None; **K. Branham**, None; **N. Khan**, None; **A. Bahr**, None; **L. Baehr**, None; **I. Magyar**, None; **S. Koller**, None; **S. Azzarello-Burri**, None; **D. Niedrist**, None; **E. Heon**, None; **W. Berger**, None

References

1. Nishimura DY, Baye LM, Perveen R, et al. Discovery and functional analysis of a retinitis pigmentosa gene, C2ORF71. *Am J Hum Genet*. 2010;86:686–695.
2. Tiwari A, Bahr A, Bahr L, et al. Next generation sequencing based identification of disease-associated mutations in Swiss patients with retinal dystrophies. *Sci Rep*. 2016;6:28755.
3. Audo I, Lancelot ME, Mohand-Said S, et al. Novel C2orf71 mutations account for approximately 1% of cases in a large French arRP cohort. *Hum Mutat*. 2011;32:E2091–E2103.
4. Collin RW, Safieh C, Littink KW, et al. Mutations in C2ORF71 cause autosomal-recessive retinitis pigmentosa. *Am J Hum Genet*. 2010;86:783–788.
5. Hebrard M, Manes G, Bocquet B, et al. Combining gene mapping and phenotype assessment for fast mutation finding in non-consanguineous autosomal recessive retinitis pigmentosa families. *Eur J Hum Genet*. 2011;19:1256–1263.
6. Bocquet B, Marzouka NA, Hebrard M, et al. Homozygosity mapping in autosomal recessive retinitis pigmentosa families detects novel mutations. *Mol Vis*. 2013;19:2487–2500.
7. Coppieters F, Van Schil K, Bauwens M, et al. Identity-by-descent-guided mutation analysis and exome sequencing in consanguineous families reveals unusual clinical and molecular findings in retinal dystrophy. *Genet Med*. 2014;16:671–680.
8. Gonzalez-del Pozo M, Mendez-Vidal C, Bravo-Gil N, et al. Exome sequencing reveals novel and recurrent mutations with clinical significance in inherited retinal dystrophies. *PLoS One*. 2014;9:e116176.

9. Katagiri S, Akahori M, Sergeev Y, et al. Whole exome analysis identifies frequent CNGA1 mutations in Japanese population with autosomal recessive retinitis pigmentosa. *PLoS One*. 2014;9:e108721.
10. Sanchez-Alcudia R, Corton M, Avila-Fernandez A, et al. Contribution of mutation load to the intrafamilial genetic heterogeneity in a large cohort of Spanish retinal dystrophies families. *Invest Ophthalmol Vis Sci*. 2014;55:7562–7571.
11. Beheshtian M, Saee Rad S, Babanejad M, et al. Impact of whole exome sequencing among Iranian patients with autosomal recessive retinitis pigmentosa. *Arch Iran Med*. 2015;18:776–785.
12. McCulloch DL, Marmor MF, Brigell MG, et al. ISCEV Standard for full-field clinical electroretinography (2015 update). *Doc Ophthalmol*. 2015;130:1–12.
13. Hood DC, Bach M, Brigell M, et al. ISCEV standard for clinical multifocal electroretinography (mfERG) (2011 edition). *Doc Ophthalmol*. 2012;124:1–13.
14. Gillingham MB, Weleber RG, Neuringer M, et al. Effect of optimal dietary therapy upon visual function in children with long-chain 3-hydroxyacyl CoA dehydrogenase and trifunctional protein deficiency. *Mol Genet Metab*. 2005;86:124–133.
15. Milam AH, Jacobson SG. Photoreceptor rosettes with blue cone opsin immunoreactivity in retinitis pigmentosa. *Ophthalmology*. 1990;97:1620–1631.
16. Zweifel SA, Engelbert M, Laud K, Margolis R, Spaide RF, Freund KB. Outer retinal tubulation: a novel optical coherence tomography finding. *Arch Ophthalmol*. 2009;127:1596–1602.
17. Schaal KB, Freund KB, Litts KM, Zhang Y, Messinger JD, Curcio CA. Outer retinal tubulation in advanced age-related macular degeneration: optical coherence tomographic findings correspond to histology. *Retina*. 2015;35:1339–1350.
18. Boulanger-Scemama E, El Shamieh S, Demontant V, et al. Next-generation sequencing applied to a large French cone and cone-rod dystrophy cohort: mutation spectrum and new genotype-phenotype correlation. *Orphanet J Rare Dis*. 2015;10:85.
19. Yang L, Cui H, Yin X, et al. Dependable and efficient clinical molecular diagnosis of chinese rp patient with targeted exon sequencing. *PLoS One*. 2015;10:e0140684.
20. Goldberg NR, Greenberg JP, Laud K, Tsang S, Freund KB. Outer retinal tubulation in degenerative retinal disorders. *Retina*. 2013;33:1871–1876.
21. Litts KM, Messinger JD, Dellatorre K, Yannuzzi LA, Freund KB, Curcio CA. Clinicopathological correlation of outer retinal tubulation in age-related macular degeneration. *JAMA Ophthalmol*. 2015;133:609–612.
22. Iriyama A, Aihara Y, Yanagi Y. Outer retinal tubulation in inherited retinal degenerative disease. *Retina*. 2013;33:1462–1465.
23. Fujinami K, Sergouniotis PI, Davidson AE, et al. Clinical and molecular analysis of Stargardt disease with preserved foveal structure and function. *Am J Ophthalmol*. 2013;156:487–501 e481.
24. Heon E, Alabduljalil T, McGuigan ID, et al. Visual function and central retinal structure in choroideremia. *Invest Ophthalmol Vis Sci*. 2016;57:OCT377–387.
25. Litts KM, Messinger JD, Freund KB, Zhang Y, Curcio CA. Inner segment remodeling and mitochondrial translocation in cone photoreceptors in age-related macular degeneration with outer retinal tubulation. *Invest Ophthalmol Vis Sci*. 2015;56:2243–2253.
26. Hildebrandt F, Benzing T, Katsanis N. Ciliopathies. *N Engl J Med*. 2011;364:1533–1543.
27. Liu YP, Bosch DG, Siemiatkowska AM, et al. Putative digenic inheritance of heterozygous RP1L1 and C2orf71 null mutations in syndromic retinal dystrophy. *Ophthalmic Genet*. 2017;127–132.
28. Deveault C, Billingsley G, Duncan JL, et al. BBS genotype-phenotype assessment of a multiethnic patient cohort calls for a revision of the disease definition. *Hum Mutat*. 2011;32:610–619.
29. Branfield Day L, Quammie C, Heon E, et al. Liver anomalies as a phenotype parameter of Bardet-Biedl syndrome. *Clin Genet*. 2015.
30. Kay BK, Williamson MP, Sudol M. The importance of being proline: the interaction of proline-rich motifs in signaling proteins with their cognate domains. *FASEB J*. 2000;14:231–241.

Investigative Ophthalmology & Visual Science